ISSN 1068-3356, Bulletin of the Lebedev Physics Institute, 2023, Vol. 50, Suppl. 5, pp. S552–S559. © Allerton Press, Inc., 2023.
Russian Text © The Author(s), 2023, published in Kvantovaya Elektronika, 2023, Vol. 53, No. 1, pp. 29–33.

## INTERACTION OF LASER RADIATION WITH MATTER. LASER PLASMA

# Electron Diffraction Study of the Structural Changes in a Thin GeTe Crystal Exposed to High-Power Femtosecond Laser Radiation

**B. N. Mironov[a,*], I. V. Kochikov[b], S. A. Aseev[a], V. V. Ionin[c], A. V. Kiselev[c], A. A. Lotin[c], S. V. Chekalin[a], A. A. Ischenko[d], and E. A. Ryabov[a,**]**

[a] *Institute of Spectroscopy, Russian Academy of Sciences, Troitsk, Moscow, 108840 Russia*

[b] *Faculty of Physics, Lomonosov Moscow State University, Moscow, 119991 Russia*

[c] *Institute of Problems of Laser and Information Technologies, Federal Scientific Research Centre "Crystallography and Photonics," Russian Academy of Sciences, Shatura, Moscow oblast, 140700 Russia*

[d] *Lomonosov Institute of Fine Chemical Technologies, Russian Technological University (MIREA), Moscow, 119571 Russia*

**e-mail: isanfemto@yandex.ru*

***e-mail: ryabov@isan.troitsk.ru*

Received October 17, 2022; revised December 20, 2022; accepted December 20, 2022

**Abstract**—The possibility of amorphization of a thin germanium telluride crystal irradiated by high-power 800-nm femtosecond laser pulses has been investigated. The sample was a 20-nm-thick film of crystalline semiconductor GeTe. An electron diffractometer with a source of short photoelectron pulses was used to study the structural changes. The electron diffraction patterns were analyzed, and the α- and β- phases have been identified in GeTe. It is established that sample ablation occurs in the strong field of femtosecond laser pulses, which is accompanied by a decrease in the crystalline phase thickness to 5–6 nm without any significant amorphization of the sample. A specific feature of the observed process—the absence of light-induced transition of a thin GeTe film from the crystalline to the amorphous state under femtosecond laser irradiation—is noted. Possible causes of the revealed effect are discussed.

**Keywords:** femtosecond laser radiation, phase-change materials, electron diffraction, thin GeTe crystal

**DOI:** 10.3103/S1068335623170086

## 1. INTRODUCTION

Binary chalcogenides of the (IV–VI)-group elements are unique materials characterized by two stable phase states (crystalline and amorphous), making it practically possible to code information based on a phase transition. Among this class of phase-change materials (PCMs), germanium telluride (GeTe) stands out; this is a semimetal and ferroelectric, with one of the simplest crystal structures. For example, under steady-state conditions, the cubic structure of the stone salt type (β phase with the space group F*m*-3*m*) is formed at temperatures of 693–973 K, depending on the sample deviation from stoichiometry. At lower temperature (in the range of 473–673 K) GeTe is crystallized with formation of a rhombohedral structure (α phase with the space group R3*m*), which is a "distorted" face-centered cubic lattice [1, 2].

The significant difference in the physical properties of the crystalline and amorphous states of a PCM can be used to develop a universal memory on their basis [3]. The phase state of such a material may change under pulses of different nature (thermal impact, electrical pulse, light) [3–5]. Reversible transitions of GeTe from the crystalline to the amorphous state and vice versa may be induced by nanosecond laser pulses [6–8]. A promising approach is the use of ultrashort laser radiation, which is expected to implement in future ultrafast information exchange in storage devices [3]. For example, the behavior of PCM $Ge_2Sb_2Te_5$ in a femtosecond laser field was investigated previously, and the possibilities of a non-thermal change in the PCM structure on the picosecond and subpicosecond scales were demonstrated [9–11].

The purpose of this work was to perform an electron diffraction study of a thin-film GeTe crystal before and after its exposure to high-power single femtosecond laser pulses, as well as to analyze the observed electron diffraction patterns. As far as we know, thin GeTe films have not been studied previously by this method.

The results obtained may be of interest from both practical and fundamental points of view. Primarily, this concerns the possibility of designing fast memory for long-term storage based on a material allowing for multiple and strictly reversible light-induced phase transitions. At the same time, a thin film of this material could be in fact an ideal sample for studying its structural dynamics with high spatial and temporal resolution by ultrafast electron diffraction (UED), using ultrashort electron pulses (pulses containing a small number of electrons) in the signal acquisition mode.

## 2. EXPERIMENTAL

Experimental data were obtained on a compact electron diffractometer using an ultrashort (~300 fs) pulsed electron beam and a highly sensitive detection scheme [12–14]. To observe the structural dynamics, the system provides a pump–probe analysis (using photoelectron bunches) of a thin-film crystalline sample irradiated by ultrashort laser pulses. A necessary condition for carrying out time-resolved measurements on this diffractometer is the acquisition of signal from a fairly large number of pulses, which, in turn, requires reversibility of the studied laser-induced phase transitions and possibility of monitoring the state of the laser-irradiated sample.

The instrument can also be used in the "classical" mode to observe static electron diffraction patterns in thin crystals. In contrast to the conventional electron diffractometer, the probe electron bunches used here are due to the photoelectric effect. A pulsed photoelectron beam is formed as a result of irradiation of a photocathode (semitransparent 20-nm-thick gold film) by the 3rd harmonic of a femtosecond Ti:sapphire master laser. In our scheme, the pulsed photoelectron beam with a kinetic energy of 36 keV, probing the target, contained ~$10^3$ electrons per pulse. The electron beam with a diameter of about 100 μm near the sample was formed by a lens based on a permanent magnet. The signal was recorded using a position-sensitive detector, consisting of two microchannel plates (MCPs) and a phosphor screen. The phosphor data were read by a CCD camera and sent to a computer for subsequent analysis. The pressure in the vacuum chamber was ~$10^{-7}$ Torr, and the sample–detector distance was about 200 mm.

The object of study was a polycrystalline 20-nm-thick GeTe sample, formed by vacuum thermal deposition on a commercially available copper mesh with a cell size of about 64 μm, coated by a 20-nm-thick carbon film (Ted Pella, Inc.). The copper meshes were purified by 3-h annealing in vacuum at a temperature of 523 K and then cooled in the chamber for 20 h. Then the copper meshes were processed by a glow discharge in vacuum for 5 min. (Note stability of the carbon film to these processes.) Then 20-nm-thick amorphous GeTe films were deposited by thermal evaporation on a copper mesh with a carbon film at room temperature. The PCM film thickness was controlled by a quartz sensor. The initial GeTe material was evaporated from a corundum crucible. To make the samples crystalline, they were annealed in vacuum at 523 K for 1 h.

Figure 1 shows an image of a thin GeTe film (recorded with an optical microscope Neophot-32), directly after the deposition on a copper mesh and after 3-h annealing at 523 K. In Fig. 1b one can see open cell windows, formed because of locally insufficient adhesion and mechanical damage of the film.

To confirm the sample crystallinity, a test GeTe film was deposited on a test rectangular glass plate with metal contacts in the same technological cycle in which the samples were fabricated. The test sample resistance was 835 MΩ, but after annealing it decreased to 380 Ω, which confirms the crystalline state of the sample [7].

The prepared thin-film GeTe crystal was placed in the vacuum chamber of the electron diffractometer, where it was irradiated by single high-power 50-fs pulses of linearly polarized 800-nm laser beam (pump channel) at an angle of 45° with the sample surface. After the end of the optical irradiation of the sample the master Ti:sapphire laser was transferred to the frequency-pulse (1 kHz) mode, the sample was probed by a pulsed electron beam formed on the cathode due to the photoelectric effect, and an electron diffraction pattern was recorded in transmission for 20 s. Then the master laser was returned to the single-pulse mode, and the pulse energy was increased (eventually, the laser pulse energy density increased up to ~40 mJ/cm$^2$; the maximum value was determined by the spurious illumination of the detector). The irradiation was performed at the same site on the sample surface, which did not exclude accumulation of changes in the sample during measurements. The choice of this approach was dictated by the limited lateral homogeneity of the sample at the level of few hundred micrometers, which is related to the difficulty of preparing spatially homogeneous GeTe nanofilms.

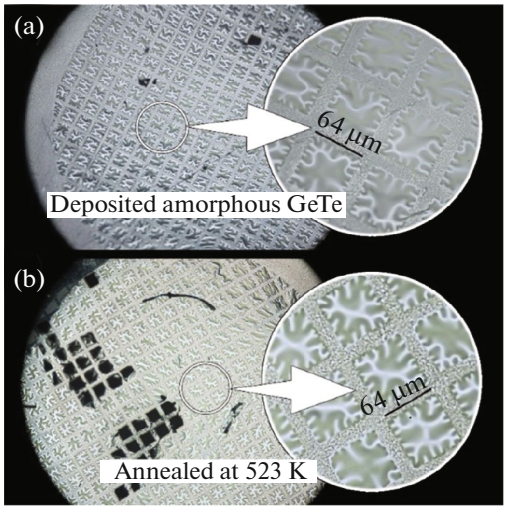


**Fig. 1.** Images of a thin GeTe film on a copper mesh, recorded (a) directly after deposition and (b) after 3-h annealing at 523 K.

## 3. MODELING OF EXPERIMENTAL DIFFRACTION PATTERNS

To interpret the experimental electron diffraction data, we modeled the distributions of diffracted-electron intensity in the detector plane. The starting information was the description of the sample crystal structure taken from the crystallographic database. Then radial intensity distributions were calculated for polycrystals.

Note that the intensity distribution for a polycrystalline structure can be calculated in different ways. The simplest one is to use the known calculation methods for calculating the electron scattering intensity in the gas electron diffraction with the only difference: a molecule is replaced with a crystallite, and the electron scattering intensity is averaged over the isotropic spatial orientations of this crystallite, similar to averaging over gas phase molecules [15].

The second way implies averaging over all directions of the diffraction pattern calculated for a crystal. Specifically, the positions of reflections and their intensities are calculated for each direction, after which averaging over all angles is performed. In this case one can choose a sufficiently large number of test points, uniformly distributed over the sphere surface, and successively orient crystal in each position. Note that both approaches give similar results.

An important circumstance is that in both cases calculation is performed within the kinematic approximation, disregarding the multiple electron scattering in the crystal. However, strictly speaking, in view of the strong elastic and inelastic electron scattering, the kinematic theory (reflecting the Born approximation of scattered wave smallness in comparison with the incident wave) is applicable to only very thin crystals. Fundamentals of the dynamic theory (considering the dynamic interaction of the primary electron beam with diffracted beams) have been developed for "thick" crystals [16]. Within the dynamic theory the two-wave approximation, which has an analytical solution, is not quite correct for the following reason: the multiwavelength mode is implemented in a "thick" crystal in practically all cases because of the strong interaction of electron with the crystal lattice. However, in practice, the use of the dynamic theory to analyze experimental data is hindered to a great extent because of the complexity of taking into account all variety of interactions of electrons with the crystal studied. Therefore, with allowance for the fact that the sample thickness decreases to 5–6 nm during the experiment, we restrict ourselves to the kinematic approximation.

## 4. RESULTS AND THEIR ANALYSIS

Figure 2 shows the electron transmission diffraction pattern of the initial 20-nm-thick GeTe film. It can be seen that the sample has a pronounced polycrystalline structure, as evidenced by a set of contrast diffraction rings. Diffraction maxima are detected against the background of smooth diffuse scattering, which is caused by thermal vibrations of crystal atoms, averaged under the experimental conditions. Note that the electron scattering from an amorphous 20-nm carbon film (the scattering amplitude decreases

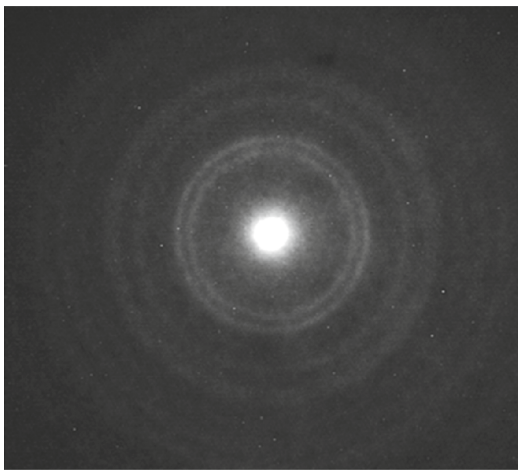

**Fig. 2.** Electron diffraction pattern of a 20-nm-thick crystalline film GeTe on a copper substrate. The observation time is 20 s, which corresponds to signal acquisition from $2 \times 10^4$ electron pulses.

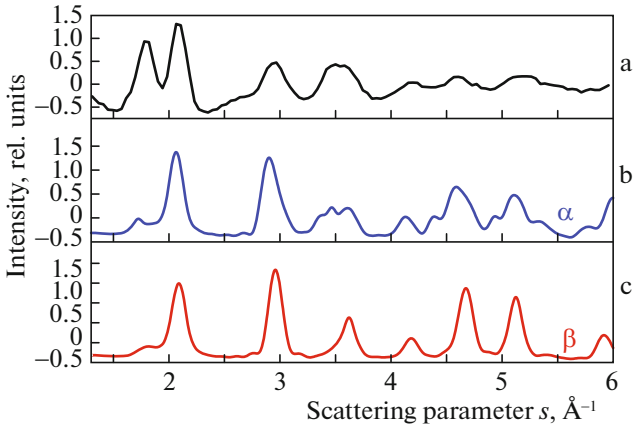


**Fig. 3.** Radial distributions of electron scattering intensity from GeTe crystals, demonstrating positions of diffraction maxima: (a) experiment and (b, c) calculation for the (b) α and (c) β phases.

with a decrease in the atomic number $Z$ of material) is negligible in comparison with the main signal from germanium telluride, without any pronounced diffraction rings.

Using the above-described model, we calculated the electron diffraction patterns of polycrystals of the α- and β-GeTe phases. The positions of reflections, as well as the sizes of diffraction rings in the screen detector, depend on the main parameters of the electron diffractometer: de Broglie wavelength ($\lambda_B$), which is ~0.064 Å for 36-keV electrons, and the sample–screen distance. The calculation results and experimental data are shown in Fig. 3. Under the chosen experimental conditions (sample–detector distance ~200 mm, detector radius ~20 mm), the recorded scattering parameter $s = (4\pi/\lambda_B)\sin(\theta/2)$, where θ is the scattering angle, lies in the range $1\ Å^{-1} < s < 6\ Å^{-1}$. The lower boundary is determined by the angular size of the screen area irradiated by the electron beam that was unscattered by the sample and arrived at the detector, and the upper boundary is determined by the entire screen size. The electrons scattered by the set of crystalline planes fall in this range (Fig. 3a). The calculated scattering intensity distributions in the cross sections of the diffraction patterns of the α- and β-GeTe phases (Fig. 3b and 3c, respectively) are also shown for comparison of the experimental and calculation results.

As follows from Fig. 3, almost all observed lines can be identified. Note that, in view of the complexity of the GeTe crystal structure, the intensity distributions contain many closely spaced rings, which cannot be resolved under experimental conditions. Table 1 contains the radii of the main diffraction rings, both recorded in the experiment and calculated for the two GeTe phases (α and β).

**Table 1.** Experimental ($R_{exp}$) and calculated ($R_{calc}$) radii of diffraction rings for the GeTe crystal*

| $R_{exp}$ (Å$^{-1}$) | $R_{cale}$ (α phase) (Å$^{-1}$) | $R_{cale}$ (β phase) (Å$^{-1}$) | $R_{exp}/R_{cale}$ (α phase) | $R_{exp}/R_{cale}$ (β phase) |
|---|---|---|---|---|
| 1.80 | 1.8094 | 1.8112 | 0.9948 | 0.9938 |
| 2.09 | 2.0670 | 2.0914 | 1.0111 | 0.9993 |
| | *2.8753* | | | |
| 2.96 | 2.9703 | 2.9577 | 0.9965 | 1.0008 |
| | *3.4379* | *3.4682* | | |
| 3.55 | 3.6187 | 3.6224 | 0.9810 | 0.9800 |
| 4.22 | 4.1340 | 4.1828 | 1.0208 | 1.0089 |
| | *4.3879* | *4.5581* | | |
| 4.65 | 4.5738 | 4.6765 | 1.0167 | 0.9943 |
| | *4.9242* | | | |
| 5.18 | 5.0905 | 5.1229 | 1.0176 | 1.0111 |
| | *5.3767* | *5.4336* | | |
| | | | 1.0055 (mean) | 0.9983 (mean) |

*The values for weak lines are given in italic.

Table 1 contains data on several weak rings for the calculated distributions; since they can barely be observed experimentally, the ratios of radii were not calculated for them. Note that all recorded diffraction rings are fairly wide, which may indicate, among other factors, the presence of amorphous state in the samples, although the data obtained correspond most closely to the joint presence of the α and β phases. As follows from Table 1, the experimental and calculated results coincide accurate to 1–2%; however, the amplitudes of recorded diffraction peaks differ significantly from the calculated ones, which requires further, more detailed analysis of the experimental data.

To find out the possibility of structural transition of a thin-film crystal to the amorphous state in a strong laser field, a GeTe sample was exposed to high-power single femtosecond pulses with $\lambda = 800$ nm, with in situ electron probing of the structure formed. The results of sample irradiation are presented in Figs. 4 and 5. Figure 4 shows the dependence of the total intensity of the diffraction pattern, including the signal corresponding to diffuse electron scattering, on the energy density $F$ of irradiating laser pulse. As follows from these data, the drop of the detector signal recorded after reaching $F \sim 35$–$40$ mJ/cm$^2$ turned out to be ~3.5, which can be explained by the ablation evaporation of the sample. Taking into account the proportionality of the integral signal to the film thickness, one can suggest a decrease in the sample thickness to 5–6 nm as a result of the laser ablation. The film formed as a result of the ablation was found to be fairly stable to the strong laser field, which may be related to the manifestation of quantum-size effects. For example, it was shown previously by an example of a thin crystal structure $MoS_2$ [17] that the ablation threshold depends on the film thickness.

As can be seen in Fig. 5, the rise of the laser pulse energy in the experiment was accompanied by a small but pronounced shift of diffraction maxima. One might suggest that this shift is caused by the change in the ratio of the α and β phases in the sample during its irradiation, because the diffraction patterns of these phases are shifted relative to each other (see Fig. 3). However, the analysis within the two-component model does not make it possible to explain completely the results obtained. Therefore, the contribution of other processes must also be taken into account. For example, one cannot exclude the occurrence of "new" phases in a GeTe crystal during laser irradiation [6].

The multiple electron scattering in a crystal ~20 nm thick may lead to intensity redistribution between Bragg peaks, which is likely one of the reasons for the inconsistency between the calculated and experimental amplitudes of diffraction pattern intensity presented in Fig. 3. However, with a decrease in the experimental sample thickness to ~6 nm after irradiation by laser pulses with $F > 25$–$30$ mJ/cm$^2$, the applicability of the kinematic approximation becomes more justified. Taking into account the fact that, even for a very thin GeTe crystal, there is a significant discrepancy between the calculation results and experimental data, which manifests itself in a difference between the diffraction peak amplitudes (in particular, at $s \approx 1.8$ and 2.1 Å$^{-1}$ (Figs. 3, 5)), there are good reasons to relate this behavior to the manifestation of the quantum-size effect in the GeTe sample [4, 5].

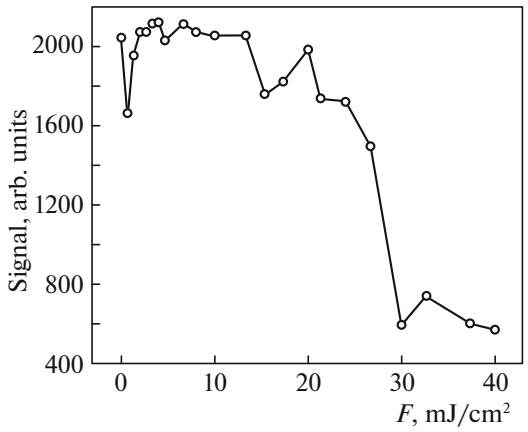


**Fig. 4.** Dependence of the total intensity of the diffraction pattern (including the diffuse electron scattering signal) on the laser fluence. The experimental data are presented as circles connected by lines for better perception.

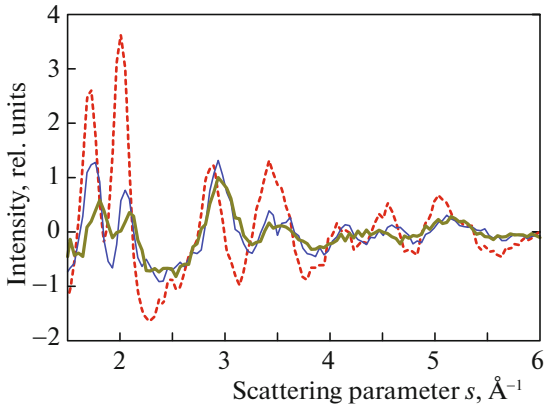


**Fig. 5.** Radial distribution profile of electron diffraction pattern intensity at different laser pulse fluences: (dashed line) prior to crystal irradiation, (thin solid line) $F \approx 27$ mJ/cm$^2$, and (bold solid line) $F \approx 34$ mJ/cm$^2$. (The scale is the same for all distributions.)

The main result of this study is the absence of a light-induced transition in GeTe from the crystalline to the amorphous state under experimental conditions. Note that, when much thicker PCM crystals and longer laser pulses are used, the behavior of GeTe becomes radically different, and there opens a possibility of implementing direct and inverse phase transitions in the material studied. For example, an initially amorphous 100-nm-thick GeTe film was exposed to 532-nm nanosecond laser pulses in [7, 8]. The GeTe crystallization began at the threshold energy density $F \approx 8$ mJ/cm$^2$. The α-GeTe fraction increased when moving deeper into the film bulk ($F \approx 19$–$32$ mJ/cm$^2$), with subsequent transition to the β phase ($F \approx 32$–$48$ mJ/cm$^2$), which was revealed by recording X-ray diffraction patterns. The inverse transition from the crystalline to the amorphous state began at $F \approx 62$ mJ/cm$^2$. These measurements were performed at fairly high laser pulse energy densities: approximately up to 90 mJ/cm$^2$ (but below the ablation threshold, which is 100 mJ/cm$^2$ or higher for nanosecond pulses).

A relatively low ablation threshold ($F \approx 30$ mJ/cm$^2$) was observed for a GeTe crystal in a femtosecond laser field; in our opinion, this may a hindrance for achieving the conditions necessary for implementing a laser-induced phase transition from the crystalline state. As was previously demonstrated when studying a thin GST crystal by the UED method [10], the femtosecond laser ablation threshold for the PCM in use turned out to be ~30 mJ/cm$^2$. Note that this value practically coincides with the results of our measurements performed on a simpler binary compound.

At the same time, the confinement in thin (thinner than 15–20 nm) GeTe films [4, 5], which affects the characteristics of material, may also be an important factor. The quantum-size effect in this com-

pound (only in the crystalline, not in the amorphous state) is due to the competition between the electron localization, corresponding to the metallic bonding, and the electron delocalization, inherent in the covalent bonding.

The consequence of this combined relationship is the entire set of properties inherent in exclusively ultrathin GeTe films. For example, broadening of the X-ray diffraction reflections observed for a thin-film crystal [5] could explain (at least, at the qualitative level) the discrepancy between the experimental data and theory predictions, when the amplitudes of measured diffraction peaks differ significantly from the calculated values. Indeed, all other factors being equal, a broadening of a diffraction peak should be accompanied by a decrease in its amplitude.

## 5. CONCLUSIONS

Thus, using a compact electron diffractometer with short electron pulses (electron energy 36 keV), we studied a thin germanium telluride crystal with the initial thickness of 20 nm. Electron diffraction patterns of a GeTe film before and after its irradiation by high-power single femtosecond laser pulses were recorded. Electron diffraction patterns were also calculated for the $\alpha$ and $\beta$ phases of GeTe, and good coincidence with the experimentally found radii of diffraction rings was obtained.

In contrast to the reversible light-induced transitions in a 100-nm-thick GeTe sample subjected to nanosecond laser irradiation, stability of the phase state in the strong field of femtosecond laser pulse was found for a 20-nm-thick crystal. The detailed analysis of the achievement of the ablation mode for GeTe without any significant amorphization of crystalline sample under these conditions is a subject of future study.

In future, to exclude the influence of quantum confinement on measurements, it is expedient to use GeTe films more than 30 nm thick, which, correspondingly, will require higher electrons energies (~60 keV), providing effective sample probing in transmission. In addition, crystalline samples with better spatial homogeneity can be prepared in this case.

## FUNDING

This study was supported by the Russian Foundation for Basic Research, project no. 20-02-00146 A, and performed on a unique scientific facility "Multipurpose Femtosecond Laser-Diagnostic Spectrometric Complex" of the Institute of Spectroscopy of the Russian Academy of Sciences and state assignment no. FFUU-2022-0004.

## CONFLICT OF INTEREST

The authors declare that they have no conflicts of interest.

## REFERENCES

1. Leger, J.M. and Redon, A.M., *J. Phys.: Condens. Matter.,* 1990, vol. 2, p. 5655.
2. Onodera, A., Sakamoto, I., and Fujii, Y., *Phys. Rev. B,* 1997, vol. 56, p. 7935.
3. Wuttig, M., Bhaskaran, H., and Taubner, T., *Nat. Photonics,* 2017, vol. 11, p. 465.
4. Kooi, B.J. and Wuttig, M., *Adv. Mater.,* 2020, vol. 32, p. 1908302.
5. Kerres, P., Zhou, Y., Vaishnav, H., Raghuwanshi, M., Wang, J., Häser, M., Pohlmann, M., Cheng, Y., Schön, C.-F., Jansen, Th., Bellin, Chr., Bürgler, D.E., Jalil, A.R., Ringkamp, Chr., Kowalczyk, H., Schneider, C.M., Shukla, Abh., and Wuttig, M., *Small,* 2022, vol. 18, p. 2201753.
6. Jeong, Kw., Park, S., Park, D., Ahn, M., Han, J., Yang, W., Jeong, H.-S., and Cho, M.-H., *Sci. Rep.,* 2017, vol. 7, p. 955.
7. Kiselev, A.V., Mikhalevsky, V.A., Burtsev, A.A., Ionin, V.V., Eliseev, N.N., Lotin, A.A., *Opt. Laser Technol.,* 2021, vol. 143, p. 107305.
8. Burtsev, A.A., Eliseev, N.N., Mikhalevsky, V.A., Kiselev, A.V., Ionin, V.V., Grebenev, V.V., Karimov, D.N., and Lotin, A.A., *Mater. Sci. Semicond. Process.,* 2022, vol. 150, p. 106907.
9. Wu, H., Han, W., and Zhang, X., *Materials,* 2022, vol. 15, p. 6760.
10. Waldecker, L., Miller, T.A., Rude, M., Bertoni, R., Osmond, J., Pruneri, V., Simpson, R., Ernstorfer, R., and Wall, S., *Nat. Mater.,* 2015, vol. 14, p. 991.
11. Qi, Y., Chen, N., Vasileiadis, Th., Zahn, D., Seiler, H., Li, X., and Ernstorfer, R., *Phys. Rev. Lett.,* 2022, vol. 129, p. 135701.

12. Mironov, B.N., Kompanets, V.O., Aseev, S.A., Ishchenko, A.A., Kochikov, I.V., Misochko, O.V., Chekalin, S.V., and Ryabov, E.A., *J. Exp. Theor. Phys.,* 2017, vol. 124, p. 422.
13. Mironov, B.N., Aseev, S.A., Ishchenko, A.A., Kochikov, I.V., Chekalin, S.V., and Ryabov, E.A., *Quantum Electron.,* 2020, vol. 50, no. 3, p. 242.
14. Aseyev, S.A., Ryabov, E.A., Mironov, B.N., Kochikov, I.V., and Ischenko, A.A., *Chem. Phys. Lett.,* 2022, vol. 797, p. 139599.
15. Ishchenko, A.A., Girichev, G.V., and Tarasov, Yu.I., *Difraktsiya elektronov: Struktura i dinamika svobodnykh molekul i kondensirovannogo sostoyaniya veshchestva* (Electron Diffraction: Structure and Dynamics of Free Molecules and Condensed Matter), Moscow: Fizmatlit, 2013.
16. Hirsch, P.B., Howie, A., Nicholson, R.B., Pashley, D.W., and Whelan, M.J., *Electron Microscopy of Thin Crystals,* Londres: Butterworths, 1965.
17. Paradisanos, I., Kymakis, E., Fotakis, C., Kioseoglou, G., and Stratakis, E., *Appl. Phys. Lett.,* 2014, vol. 105, p. 041108.

*Translated by Yu. Sin'kov*